Density Functional Theory and the Correlation Consistent Basis Sets: The Tight *d* Effect on HSO and HOS

Nick X. Wang and Angela K. Wilson*

Department of Chemistry, University of North Texas, Denton, Texas 76203-5070

Received: September 27, 2004; In Final Form: April 20, 2005

The HSO and HOS isomers have been revisited using the DFT functionals, B3LYP, B3PW91, and PBE, in combination with tight *d*-augmented correlation consistent basis sets, cc-pV(x+d)Z and aug-cc-pV(x+d)Z for second-row atoms. Structures, vibrationally averaged structures, relative energies, harmonic and anharmonic frequencies, enthalpies of formation of HSO and HOS, and the barrier for the HSO/HOS isomerization have been determined. These results were compared with results from previous DFT and ab initio studies in which the standard correlation consistent basis sets were used. The relative energies of the two isomers converge more rapidly and smoothly with respect to increasing basis set size for the tight *d*-augmented sets than for the standard basis sets. Our best calculations, B3PW91/aug-cc-pV(5+*d*)Z, for the relative energy of the isomers are in excellent agreement with previous CCSD(T) results given by Wilson and Dunning.

I. Introduction

The correlation consistent basis sets have been shown in thousands of studies reported in the literature to be important in the high accuracy description of molecular properties and energetics.[1−12] One of the early successes of the correlation consistent basis sets was for the HSO and HOS isomers. All prior theoretical studies had predicted that HOS was the more stable of the two isomers,[13−16] while experiments had predicted the HSO isomer to be more stable.[17,18] In 1993, Xantheas and Dunning carried out two studies on these species,[19,20] and by using more advanced methodology (CASSCF) in combination with correlation consistent basis sets of at least triple-ζ quality correctly predicted HSO to be the more stable isomer.

Since this time, the correlation consistent basis sets have been well utilized in numerous studies of sulfur species. The systematic, convergent behavior of the basis set family—toward the complete basis set (CBS) limit—has proven to be a tremendous aid in high accuracy calculations and in helping to establish a hierarchy of computational methods. Despite the successes, a study by Bauschlicher and Partridge done in 1995 indicated a possible flaw with the basis set family for sulfur.[21] The focus of Bauschlicher's study was the binding energy of SO_2. They used a series of three basis sets—cc-pVTZ, cc-pVQZ, and cc-pV5Z—in combination with CCSD(T)[22,23] to extrapolate the binding energy to the CBS limit. Upon extrapolation, the binding energy was still 6 kcal/mol from a well-established experiment—far from the desired "chemical accuracy" of 1 kcal/mol. They noted that the addition of tight *d* functions to the basis sets for sulfur helped to reduce the error.

Martin also examined the unusual basis set behavior for sulfur species by studying the atomization energies, geometries, and spectroscopic properties of SO and SO_2.[24] He suggested that the addition of (1*d*), (2*d*1*f*), and (3*d*2*f*1*g*) functions to the cc-pVTZ, cc-pVQZ, and cc-pV5Z basis sets, respectively, for sulfur would lead to improved results when a Schwartz-type extrapolation scheme was used for SO_2. In later studies, he also recommended these basis set modifications for SO and SO_3, while in studies with Uzan,[25] he suggested that such an approach also be used to calculate dissociation energies, geometries, and spectroscopic constants of other second row species.

Dunning, Peterson, and Wilson examined the observed deficiencies in the basis sets.[12] They noted that care must be taken in the modification of the correlation consistent basis sets, as any addition to the basis sets would lead to improvement in the total energy as well as to the dissociation energy as correlation effects are usually more pronounced in molecules than in atoms. A result of this study was the modification of the second-row basis sets, resulting in the cc-pV(x+d)Z and aug-cc-pV(x+d)Z basis sets, which included a tight *d* function at each basis set level (as well as modifications to the standard set of *d* functions) to help improve the results obtained for species such as sulfur, while still maintaining the convergent behavior of the correlation consistent basis sets. Such dramatic improvements in energies occurred with a minimal increase in computational cost, as the tight *d*-augmented basis sets only increase the total number of basis functions in the standard basis set by five functions for each level of basis set.

The revised basis sets have been used in a number of benchmark studies predominantly by Wilson and co-authors.[1,12,26−28] The studies have focused largely on the effects of the new basis sets in combination with CCSD(T) upon the dissociation energies and structures of species such as SO, SO_2, and SO_3. Work by Wang and Wilson examined the impact of the basis sets upon such properties when combined with density functional theory (DFT) for SO_2, CCl, and ClO_2.[26] In all of these studies, the effect of tight *d* functions is quite substantial, particularly at the double-ζ and triple-ζ levels for the sulfur species, with improvements in dissociation energies as large as 25 kcal/mol. Overall, the convergence behavior toward the CBS limit (or the Kohn−Sham limit, in the case of DFT) is also substantially improved.

A recent study by Wilson and Dunning revisited the HSO and HOS isomers.[1] They found that the tight *d* functions enabled the correct prediction of the greater stability of the HSO isomer with a lower level basis set when combined with CCSD(T) than

* Corresponding author e-mail: akwilson@unt.edu.

10.1021/jp045622b CCC: $30.25
Published on Web 07/27/2005

with the regular correlation consistent basis sets. In an early study of the HSO and HOS isomers, Denis and Ventura focused upon the enthalpies of formation of the two species using density functional methods (B3LYP and B3PW91) in combination with the regular and augmented correlation consistent basis sets.[29] They noted a remarkable agreement with experiment and calculations using higher-level basis sets. Though there have been numerous studies of the HSO and HOS isomers,[30−32] other particularly noteworthy studies are those by Marshall et al.[33] and Schaefer et al.[34]

In the current study, we revisit the HSO and HOS isomers with DFT and examine the performance of the revised basis sets not only upon the relative energies of the two species but also upon the thermochemistry. This is the first density functional benchmark study on the impact of the tight *d* species upon the enthalpies of formation of sulfur species.

II. Computational Details

Three functionals, B3LYP,[35,36] B3PW91,[37] and PBE,[38,39] were used in the calculations and were combined with the two new families of correlation consistent basis sets: cc-pV(x+d)Z and aug-cc-pV(x+d)Z. For the PBE functional, calculations were also performed using the cc-pVxZ and aug-cc-pVxZ basis sets. All calculations were performed using the Gaussian 98 and Gaussian 03 program suites.[40,41] Geometry optimizations and frequency calculations were done for each functional and basis set combination. Zero point energy corrections were taken directly from the frequency calculations without scaling and were included in the final energies reported. To evaluate the density functional integrals, the default numerical grid (75 302) provided in the Gaussian program was used. This grid includes 75 radial shells and 302 angular points per shell, resulting in approximately 7000 quadrature points per atom. In general, this grid is known to provide energies accurate to five places past the decimal.

The Gaussian 03 program suite was used to determine the vibrational averaged structures and anharmonic frequencies via numerical differentiation along the normal modes.[42−45] Calculations to obtain the anharmonic properties were done for all three density functionals in combination with both the standard and tight *d*-augmented correlation consistent basis sets. The SURFIT program[46] was used to confirm the anharmonic frequencies obtained. For each molecule, a total of 125 points was calculated in a range of $0.4a_o \geq \Delta r \geq -0.4a_o$ and $40° \geq \theta \geq -40°$. Spectroscopic parameters were determined from the potential curve generated by these points. The anharmonic frequencies obtained are similar to those determined using Gaussian 03, with slight differences of no more than a few wavenumbers.

Two schemes have been used to extrapolate the energetic results obtained from calculations using a series of the correlation consistent basis sets to the Kohn−Sham limit. The first approach is the exponential scheme:

$$D_e(x) = D_e(\infty) + Ae^{-Bx}$$

This approach has been used extensively to approximate CBS limits for ab initio methods such as HF, MP2, CISD, and CCSD(T) since Feller first introduced the scheme in 1992.[47] More recently, the scheme has been used successfully to approximate Kohn−Sham (KS) limits for a number of density functional methods.[48−50] Within the extrapolation scheme, x is the cardinal number of the basis set (i.e. for cc-pVDZ, x=2; for cc-pVTZ, x=3), $D_e(x)$ represents the energy at the "x" level, and $D_e(\infty)$ represents the extrapolated energy at the CBS limit or KS limit in the case of DFT. A and B are parameters that are determined in the fit. Using this scheme, at least three data points are necessary. In this study, two exponential fits were used to obtain the KS limits. The first, denoted KS_{DTQ5}, includes four data points, where "D" represents the data obtained using a double-ζ level basis set, "T" represents the triple-ζ level, "Q" represents the quadruple-ζ level, and "5" represents the quintuple-ζ level. The second, denoted KS_{DTQ}, includes results from double-, triple-, and quadruple-ζ level basis sets.

Another commonly used extrapolation scheme is a two-point extrapolation approach introduced by Halkier et al.[51] The formulation is as follows:

$$D_e(\infty) = \frac{(D_e(x) \times x^3) - (D_e(x-1) \times (x-1)^3)}{x^3 - (x-1)^3}$$

For this scheme, three extrapolations were done: KS_{DT}, KS_{TQ}, and KS_{Q5} where "DT" refers to the inclusion of double- and triple-ζ level results in the fit and similarly for the other pairings. Again, x represents the cardinal number of the basis set.

III. Results and Discussion

A. Structures of the HSO and HOS Isomers. Optimized structures and vibrationally averaged structures obtained using B3LYP, B3PW91, and PBE in combination with the cc-pV(x+d)Z and aug-cc-pV(x+d)Z basis sets are provided in Tables 1 and 2. To examine the overall impact of the tight *d*-augmented basis sets, results from Denis and Ventura's earlier study[29] using the standard correlation consistent basis sets are included in Table 1 for comparison for B3LYP and B3PW91. As shown in the tables, the bond lengths of H−S and S−O for HSO and S−O for HOS converge more rapidly when the tight *d*-augmented basis sets are used than for the standard correlation consistent basis sets. For example, the bond length of S−O in HSO, which experiences the greatest impact, is nearly converged at the cc-pV(T+d)Z level, while with the standard basis sets, the bond length does not approach convergence until the cc-pVQZ or cc-pV5Z level. The effect upon the S−H bond length in HSO is minimal, with the greatest difference of 0.004 Å at the double-ζ level for PBE. Additional diffuse functions (aug-cc-pV(x+d)Z) result in a small difference in the bond lengths as compared with those obtained using the regular tight *d*-augmented basis sets (cc-pV(x+d)Z), with differences ranging from 0.001 to 0.007 Å. In general, cc-pV(T+d)Z structures are similar to those obtained using the cc-pVQZ or cc-pV5Z basis sets.

Overall, the bond angles are affected very slightly (<1.0°) by the tight *d* functions, with the greater impact occurring for the smaller basis sets. Interestingly, the HSO bond angle increases for the cc-pVxZ series as the basis set size increases, while it decreases for cc-pV(x+d)Z when the basis set size increases. The opposite trend occurs for the HOS angle.

In comparing B3LYP and B3PW91, both result in nearly identical structures. Both methods are in good agreement with experimental geometries for HSO,[52] with a converged bond distance for S−H in error from experiment by 0.015 Å for B3LYP and for B3PW91 and the S−O bond distance differing by 0.006 Å for B3LYP and in agreement with experiment for B3PW91. The bond angle differs from experiment by ∼2.0°. In comparing previous studies shown in Table 1, such as work by Wilson and Dunning which used CCSD(T) in combination with regular and tight *d* correlation consistent basis sets,[1] the calculated bond angle of the present study is in near agreement, just slightly below 105°. PBE predicts slightly longer bond

TABLE 1: Optimized Geometries for HSO and HOS[f]

		HSO			HOS		
method	basis set	r(SH), Å	r(SO), Å	θ (HSO), °	r(SO), Å	r(OH), Å	θ (HOS), °
B3LYP	cc-pVDZ	1.393	1.554	103.91	1.673	0.974	106.92
	cc-pVTZ[a]	1.379	1.518	104.24	1.648	0.967	108.42
	cc-pVQZ[a]	1.376	1.509	104.47	1.642	0.966	108.89
	cc-pV5Z[a]	1.375	1.502	104.60	1.638	0.966	109.20
	cc-pV(D+*d*)Z	1.390	1.527	104.79	1.657	0.974	107.49
	cc-pV(T+*d*)Z	1.376	1.504	104.77	1.640	0.967	108.74
	cc-pV(Q+*d*)Z	1.374	1.502	104.68	1.638	0.966	109.08
	cc-pV(5+*d*)Z	1.374	1.500	104.57	1.637	0.965	109.25
	aug-cc-pV(D+*d*)Z	1.383	1.528	103.93	1.661	0.971	108.60
	aug-cc-pV(T+*d*)Z	1.374	1.505	104.45	1.640	0.967	109.15
	aug-cc-pV(Q+*d*)Z	1.374	1.501	104.50	1.638	0.966	109.25
	aug-cc-pV(5+*d*)Z	1.374	1.500	104.54	1.637	0.966	109.29
B3PW91	cc-pVDZ	1.390	1.546	103.92	1.663	0.973	106.77
	cc-pVTZ[a]	1.378	1.512	104.29	1.639	0.965	108.16
	cc-pVQZ[a]	1.376	1.503	104.47	1.633	0.964	108.60
	cc-pV5Z[a]	1.375	1.496	104.69	1.629	0.964	108.88
	cc-pV(D+*d*)Z	1.387	1.520	104.76	1.648	0.973	107.25
	cc-pV(T+*d*)Z	1.376	1.498	104.70	1.630	0.966	108.44
	cc-pV(Q+*d*)Z	1.375	1.495	104.73	1.629	0.965	108.72
	cc-pV(5+*d*)Z	1.374	1.494	104.73	1.628	0.965	108.86
	aug-cc-pV(D+*d*)Z	1.382	1.521	104.10	1.651	0.969	108.29
	aug-cc-pV(T+*d*)Z	1.375	1.500	104.60	1.631	0.966	108.77
	aug-cc-pV(Q+*d*)Z	1.374	1.495	104.67	1.629	0.965	108.86
	aug-cc-pV(5+*d*)Z	1.374	1.494	104.71	1.628	0.965	108.89
PBE	cc-pVDZ	1.412	1.560	104.83	1.687	0.984	105.49
	cc-pVTZ	1.398	1.528	104.79	1.662	0.977	106.97
	cc-pVQZ	1.395	1.520	104.87	1.656	0.976	107.46
	cc-pV5Z	1.393	1.513	105.01	1.652	0.976	107.79
	cc-pV(D+*d*)Z	1.408	1.535	105.59	1.671	0.984	106.08
	cc-pV(T+*d*)Z	1.395	1.515	105.18	1.653	0.977	107.38
	cc-pV(Q+*d*)Z	1.393	1.512	105.08	1.652	0.976	107.65
	cc-pV(5+*d*)Z	1.392	1.512	105.04	1.651	0.976	107.83
	aug-cc-pV(D+*d*)Z	1.399	1.538	104.36	1.674	0.980	107.24
	aug-cc-pV(T+*d*)Z	1.392	1.516	104.87	1.653	0.977	107.81
	aug-cc-pV(Q+*d*)Z	1.392	1.513	104.95	1.652	0.976	107.87
	aug-cc-pV(5+*d*)Z	1.392	1.512	105.00	1.651	0.976	107.89
CASSCF[b]	aug-cc-pVDZ	1.361	1.571	103.40	1.690	0.973	105.50
	cc-pVTZ	1.355	1.528	104.69	1.656	0.969	106.34
	cc-pVQZ	1.354	1.519	104.86	1.650	0.968	106.79
CASSCF+1+2[b]	cc-pVTZ	1.363	1.518	104.75	1.655	0.965	105.81
	cc-pVQZ	1.361	1.506	104.95	1.645	0.963	106.37
CCSD(T)[c]	cc-pVDZ	1.383	1.559	103.53	1.683	0.972	105.65
	cc-pVTZ	1.371	1.517	104.32	1.648	0.965	106.94
	cc-pVQZ	1.369	1.504	104.47	1.639	0.964	107.82
	cc-pV(D+*d*)Z	1.379	1.532	104.42	1.668	0.972	106.14
	cc-pV(T+*d*)Z	1.369	1.504	104.82	1.641	0.965	107.21
	cc-pV(Q+*d*)Z	1.369	1.498	104.69	1.635	0.964	107.83
exp[d]		1.389 ± 0.005	1.494 ± 0.005	106.6 ± 0.5			
exp[e]		1.35	1.54	102			

[a] Reference 29. [b] Reference 20 [c] Reference 1. [d] Reference 52. [e] Reference 57. [f] Bond angles are in degrees and bond lengths are in angstroms.

lengths for S−H and S−O, differing by 0.003 Å and 0.018 Å, respectively, from experiment. The bond angle of H−S−O is underestimated by ∼1.6°.

The vibrationally averaged structures of HSO and HOS have also been determined and are provided in Table 2. When the dynamic correction is considered, the error as compared with experiment for the S−H bond distance is decreased to 0.001 Å for B3LYP and B3PW91, while the error of the S−O bond distance is increased to 0.01 Å for B3LYP and 0.005 Å for B3PW91. The error in the bond angle is decreased to ∼1.7°. For PBE, the dynamic correction increases the error of the S−H and S−O bond distances to 0.021 Å and 0.022 Å, respectively, while it decreases the error of the bond angle to ∼1.4°.

B. Vibrational Frequencies. As shown in Table 3, the tight *d*-augmented basis sets result in very little change in the computed vibrational frequencies as compared with the standard correlation consistent basis sets. For example, the frequency corresponding to the S−O stretch of HSO results in a value of 944 cm^{-1} with the cc-pVDZ basis set, while it is 973 cm^{-1} with the cc-pV(D+*d*)Z basis set for B3LYP. The convergence, however, is faster with the tight *d*-augmented basis sets. As shown for the S−O stretch of HSO, the B3LYP/cc-pV5Z frequency is identical to that of the B3LYP/cc-pV(T+*d*)Z frequency (which is essentially converged).

As compared to experiment, the converged B3LYP/cc-pV(*x*+*d*)Z S−O stretch frequencies (generally occurring at the triple-ζ level) are within a few wavenumbers of experiment (1013, 1026 cm^{-1}).[52,57] For B3PW91, the calculated value of 1033 cm^{-1} is just slightly above the two experimental predictions, whereas PBE predicts a value of 998 cm^{-1}, which is lower than experiment. The H−S−O bend has been calculated as 1092 cm^{-1} (B3LYP/cc-pV(T+*d*)Z) and 1106 cm^{-1} (B3PW91/cc-pV(T+*d*)Z), falling between the experimental frequencies (1063, 1164 cm^{-1}),[52,57] while the PBE/cc-pV(T+*d*)Z result of 1057

TABLE 2: Vibrationally Averaged Geometries for HSO and HOS[a]

		HSO			HOS		
method	basis set	r(SH), Å	r(SO), Å	θ (HSO), °	r(SO), Å	r(OH), Å	θ (HOS), °
B3LYP	cc-pVDZ	1.409	1.559	104.10	1.678	0.985	107.27
	cc-pVTZ	1.395	1.523	104.38	1.653	0.978	108.70
	cc-pVQZ	1.392	1.514	104.58	1.647	0.976	109.16
	cc-pV5Z	1.390	1.506	104.80	1.642	0.976	109.56
	cc-pV(D+*d*)Z	1.405	1.532	105.01	1.663	0.985	107.81
	cc-pV(T+*d*)Z	1.392	1.509	104.95	1.645	0.978	109.01
	cc-pV(Q+*d*)Z	1.391	1.506	104.83	1.643	0.976	109.34
	cc-pV(5+*d*)Z	1.390	1.505	104.85	1.642	0.976	109.52
	aug-cc-pV(D+*d*)Z	1.398	1.533	104.17	1.666	0.982	108.82
	aug-cc-pV(T+*d*)Z	1.390	1.509	104.64	1.646	0.978	109.44
	aug-cc-pV(Q+*d*)Z	1.390	1.505	104.85	1.643	0.977	109.52
	aug-cc-pV(5+*d*)Z	1.390	1.505	104.85	1.642	0.976	109.52
B3PW91	cc-pVDZ	1.406	1.551	104.14	1.653	0.984	107.54
	cc-pVTZ	1.395	1.516	104.47	1.635	0.977	108.68
	cc-pVQZ	1.392	1.507	104.70	1.633	0.975	108.95
	cc-pV5Z	1.390	1.500	104.88	1.633	0.975	109.09
	cc-pV(D+*d*)Z	1.402	1.525	104.93	1.653	0.984	107.52
	cc-pV(T+*d*)Z	1.391	1.503	104.89	1.635	0.977	108.67
	cc-pV(Q+*d*)Z	1.390	1.500	104.93	1.634	0.975	108.95
	cc-pV(5+*d*)Z	1.390	1.499	104.93	1.633	0.975	109.09
	aug-cc-pV(D+*d*)Z	1.397	1.525	104.32	1.656	0.980	108.47
	aug-cc-pV(T+*d*)Z	1.390	1.503	104.79	1.636	0.977	109.00
	aug-cc-pV(Q+*d*)Z	1.390	1.500	104.87	1.633	0.976	109.09
	aug-cc-pV(5+*d*)Z	1.390	1.499	104.91	1.633	0.975	109.13
PBE	cc-pVDZ	1.431	1.565	105.01	1.692	0.996	105.76
	cc-pVTZ	1.416	1.533	104.98	1.667	0.988	107.19
	cc-pVQZ	1.413	1.524	105.08	1.662	0.987	107.66
	cc-pV5Z	1.410	1.518	105.21	1.657	0.987	108.01
	cc-pV(D+*d*)Z	1.427	1.539	105.77	1.677	0.996	106.34
	cc-pV(T+*d*)Z	1.412	1.520	105.37	1.658	0.988	107.60
	cc-pV(Q+*d*)Z	1.410	1.517	105.29	1.657	0.987	107.86
	cc-pV(5+*d*)Z	1.410	1.516	105.24	1.656	0.987	108.05
	aug-cc-pV(D+*d*)Z	1.416	1.542	104.58	1.679	0.992	107.39
	aug-cc-pV(T+*d*)Z	1.409	1.521	105.06	1.658	0.988	108.03
	aug-cc-pV(Q+*d*)Z	1.409	1.517	105.16	1.657	0.987	108.08
	aug-cc-pV(5+*d*)Z	1.409	1.516	105.20	1.656	0.987	108.10

[a] Bond angles are in degrees and bond lengths are in angstroms.

cm^{-1} is slightly below the experimental values. For the S−H stretch of HSO, the B3LYP/cc-pV(T+*d*)Z, B3PW91/cc-pV(T+*d*)Z, and PBE/cc-pV(T+*d*)Z predictions of 2408, 2430, and 2301 cm^{-1}, respectively, are within the experimental values (2271, 2570 cm^{-1}).[52,57] For the anharmonic frequencies reported in Table 4, all were decreased by ∼10 cm^1 for the S−O stretch and the H−S−O bend and ∼150 cm^{-1} for the S−H stretch as compared with the harmonic frequencies.

Overall, as shown by the comparison of frequencies given in Table 3, there is little fluctuation in the values obtained from B3LYP, B3PW91, and CCSD(T).

C. Relative Energies of HSO and HOS. In Table 5, relative energy differences between the HSO and HOS isomers calculated with B3LYP, B3PW91, and PBE in combination with the cc-pV(*x*+*d*)Z and aug-cc-pV(*x*+*d*)Z basis set series are provided. Additionally, for comparison, previous B3LYP and B3PW91 results of Dennis and Ventura,[29] CASSCF results of Xantheas and Dunning,[20] and CCSD(T) results of Wilson and Dunning[1] have been given.

For the zero-point corrected relative energy, ΔE_o, B3LYP, B3PW91, and PBE incorrectly predict that HOS is the more stable isomer when a cc-pVDZ basis set is used. Using a cc-pVTZ basis set or larger results in the prediction that HSO is the more stable isomer. Combining these methods with a cc-pV(*x*+*d*)Z level of basis sets results in the correct prediction, even at the double-ζ level, that HSO is the more stable isomer. In earlier work by Wilson and Dunning with CCSD(T), even the tight *d*-augmented sets did not result in the correct qualitative picture at the double-ζ level.

The tight *d* functions have a significant impact on the small basis sets, in particular. For example, B3LYP/cc-pVDZ yields a ΔE_o of −2.41 kcal/mol, while cc-pV(D+*d*)Z results in 1.36 kcal/mol—an energy difference of 3.77 kcal/mol, which also results in a change in qualitative picture. The diffuse functions (aug-cc-pV(*x*+*d*)Z) increase this difference by another 1.29 kcal/mol to a ΔE_o of 2.65 kcal/mol. For the larger basis sets, the differences are less pronounced with differences of 1.41 kcal/mol between B3LYP/cc-pVQZ (ΔE_o of 3.20 kcal/mol) and B3LYP/cc-pV(Q+*d*)Z (ΔE_o of 4.61 kcal/mol) and 0.28 kcal/mol between B3LYP/cc-pV5Z (ΔE_o of 4.64 kcal/mol) and B3LYP/cc-pV(5+*d*)Z (ΔE_o of 4.92 kcal/mol).

The tight *d*-augmented sets result in much faster convergence toward a limit, as shown in Table 5. For B3LYP, the difference in the ΔE_o obtained occurring between the cc-pVQZ (3.20 kcal/mol) and cc-pV5Z (4.64 kcal/mol) basis sets is still 1.44 kcal/mol (31% of the cc-pV5Z ΔE_o), where the tight *d*-augmented sets result in a difference in the ΔE_o of only 0.31 kcal/mol (6% of the cc-pV(5+*d*)Z ΔE_o), between the cc-pV(Q+*d*)Z (4.61 kcal/mol) and cc-pV(5+*d*)Z (4.92 kcal/mol) basis sets. The B3PW91 and PBE results are very similar to these B3LYP results. In comparing previous results, similar improvement in convergence behavior is noted for CCSD(T) in combination with the correlation consistent basis sets,[1] though with overall slower convergence (49% and 17% using the types of comparisons discussed above).

Our best results for ΔE_o, 5.59 kcal/mol for B3PW91/aug-cc-pV(5+*d*)Z and 4.98 kcal/mol for B3LYP/aug-cc-pV(5+*d*)Z, can be compared with the CASSCF+1+2 and then extrapolated

TABLE 3: Harmonic Vibrational Frequencies (in cm^{-1}) for HSO and HOS

		HSO			HOS		
method	basis set	ω_1 (SO str)	ω_2 (HSO bend)	ω_3 (HS str)	ω_1 (SO str)	ω_2 (HOS bend)	ω_3 (OH str)
B3LYP	cc-pVDZ	944	1049	2394	828	1148	3702
	cc-pVTZ[a]	999	1080	2399	841	1176	3746
	cc-pVQZ[a]	1010	1088	2404	841	1174	3746
	cc-pV5Z[a]	1018	1093	2418	842	1170	3749
	cc-pV(D+*d*)Z	973	1068	2388	830	1150	3697
	cc-pV(T+*d*)Z	1018	1092	2408	845	1176	3745
	cc-pV(Q+*d*)Z	1019	1093	2419	843	1173	3747
	cc-pV(5+*d*)Z	1021	1095	2419	842	1169	3750
	aug-cc-pV(D+*d*)Z	977	1066	2426	824	1159	3737
	aug-cc-pV(T+*d*)Z	1016	1092	2424	840	1168	3741
	aug-cc-pV(Q+*d*)Z	1019	1095	2419	841	1168	3746
	aug-cc-pV(5+*d*)Z	1020	1096	2420	841	1169	3750
B3PW91	cc-pVDZ	966	1059	2428	849	1150	3736
	cc-pVTZ[a]	1016	1092	2422	865	1179	3776
	cc-pVQZ[a]	1025	1099	2423	864	1176	3775
	cc-pV5Z[a]	1032	1106	2437	864	1173	3777
	cc-pV(D+*d*)Z	994	1078	2422	851	1153	3728
	cc-pV(T+*d*)Z	1033	1106	2430	867	1181	3770
	cc-pV(Q+*d*)Z	1033	1106	2435	866	1178	3768
	cc-pV(5+*d*)Z	1034	1108	2438	866	1175	3771
	aug-cc-pV(D+*d*)Z	996	1077	2452	846	1164	3762
	aug-cc-pV(T+*d*)Z	1030	1105	2442	864	1174	3764
	aug-cc-pV(Q+*d*)Z	1033	1107	2438	864	1175	3768
	aug-cc-pV(5+*d*)Z	1033	1108	2439	865	1175	3770
PBE	cc-pVDZ	947	1014	2266	800	1102	3574
	cc-pVTZ	984	1045	2295	814	1136	3625
	cc-pVQZ	990	1051	2302	814	1133	3623
	cc-pV5Z	996	1058	2313	815	1130	3625
	cc-pV(D+*d*)Z	973	1032	2272	802	1103	3572
	cc-pV(T+*d*)Z	998	1057	2301	819	1137	3621
	cc-pV(Q+*d*)Z	998	1059	2313	817	1133	3622
	cc-pV(5+*d*)Z	998	1060	2315	816	1130	3625
	aug-cc-pV(D+*d*)Z	963	1031	2329	799	1116	3610
	aug-cc-pV(T+*d*)Z	993	1056	2322	816	1129	3616
	aug-cc-pV(Q+*d*)Z	996	1059	2319	815	1129	3622
	aug-cc-pV(5+*d*)Z	997	1060	2317	815	1129	3624
CASSCF[b]	aug-cc-pVDZ	941	1094	2634	795	1220	3692
	cc-pVTZ	959	1121	2620	820	1230	3723
	cc-pVQZ	939	1115	2651	802	1226	3713
CASSCF+1+2[b]	cc-pVTZ	1013	1099	2525	844	1220	3806
	cc-pVQZ	966	1078	2620	821	1202	3729
CCSD(T)[c]	cc-pVDZ	918	1054	2464	807	1172	3768
	cc-pVTZ	1008	1089	2452	847	1200	3792
	cc-pV(D+*d*)Z	948	1075	2458	811	1175	3766
	cc-pV(T+*d*)Z	1027	1102	2448	851	1200	3791
exp[d]		1026	1164	2271			
exp[e]		1013	1063	2570			

[a] Reference 29. [b] Reference 20. [c] Reference 1. [d] Reference 52. [e] Reference 57.

result of 5.4 kcal/mol by Xantheas and Dunning.[20] PBE/aug-cc-pV(5+*d*) provides a ΔE_o of 6.99 kcal/mol, which is 1.59 kcal/mol larger than the CASSCF+1+2. A more recent theoretical ΔE_o has been reported by Wilson and Dunning using CCSD(T) with the tight *d*-augmented sets.[1] They reported a CBS limit of 4.2 kcal/mol, which is 1.2 kcal/mol lower than that estimated by Xantheas and Dunning and is 1.7 kcal/mol higher than that (2.5 kcal/mol) determined by Esseffar using QCISD-(T)/6-311+G(5*d2f*, 2*p*).[31] In contrasting these methods, DFT may not be an ideal choice of methodology due to the multireference character of HSO. However, the current results are comparable with a number of previous results using advanced ab initio methods.[1,19,31]

As discussed in section II, several extrapolation methods have been used to estimate Kohn−Sham limits for ΔE_o, and the results are listed in Table 6. For the standard correlation consistent basis sets, the KS limits are inconsistent, depending highly upon the extrapolation scheme chosen. When the tight *d*-augmented sets are used, the KS limits show much less dependence upon the extrapolation scheme. The largest deviation occurs for the KS_{DT} extrapolation, which is to be expected. Similar KS limits are obtained whether the exponential KS_{DTQ5} or KS_{DTQ} fits or the two-point KS_{TQ} fit are used. The KS limits from the KS_{Q5} fit are slightly (∼0.2−0.5 kcal/mol) higher than those obtained using the KS_{DTQ5}, KS_{DTQ}, and KS_{TQ} extrapolation schemes. As compared with the CBS limits of 5.41 and 5.42 kcal/mol for CASSCF and CASSCF+1+2, respectively, reported by Xantheas and Dunning, the B3PW91 KS_{DTQ5}, KS_{DTQ}, and KS_{TQ} limits for aug-cc-pV(*x*+*d*)Z are in good agreement (5.54, 5.45, and 5.55 kcal/mol), while B3LYP underestimates (4.94, 4.86, and 4.97 kcal/mol) them. The KS limits for PBE overestimate these previous results. However, all of the KS limits greatly overestimate the CBS limit of 4.2 kcal/mol predicted using CCSD(T).

In Figure 1, the calculated ΔE_o for B3PW91 with respect to cc-pV(*x*+*d*)Z and aug-cc-pV(*x*+*d*)Z basis sets is shown. Included in this figure are previous cc-pV*x*Z results from Denis

TABLE 4: Anharmonic Vibrational Frequencies (in cm^{-1}) for HSO and HOS

		HSO			HOS		
method	basis set	ν_1 (SO str)	ν_2 (HSO bend)	ν_3 (HS str)	ν_1 (SO str)	ν_2 (HOS bend)	ν_3 (OH str)
B3LYP	cc-pVDZ	929	1028	2218	815	1123	3501
	cc-pVTZ	985	1062	2254	829	1146	3551
	cc-pVQZ	996	1071	2271	828	1138	3549
	cc-pV5Z	1008	1079	2283	832	1133	3549
	cc-pV(D+*d*)Z	956	1048	2223	818	1123	3496
	cc-pV(T+*d*)Z	1003	1075	2263	833	1145	3547
	cc-pV(Q+*d*)Z	1007	1078	2279	832	1137	3549
	cc-pV(5+*d*)Z	1010	1080	2286	831	1133	3551
	aug-cc-pV(D+*d*)Z	965	1050	2275	811	1128	3533
	aug-cc-pV(T+*d*)Z	1003	1076	2283	829	1137	3543
	aug-cc-pV(Q+*d*)Z	1009	1079	2284	830	1132	3547
	aug-cc-pV(5+*d*)Z	1009	1080	2287	830	1132	3552
B3PW91	cc-pVDZ	954	1045	2251	871	1135	3532
	cc-pVTZ	1006	1078	2270	872	1154	3574
	cc-pVQZ	1016	1085	2284	862	1145	3573
	cc-pV5Z	1027	1094	2297	856	1140	3574
	cc-pV(D+*d*)Z	981	1065	2251	838	1129	3533
	cc-pV(T+*d*)Z	1023	1092	2285	856	1150	3574
	cc-pV(Q+*d*)Z	1026	1093	2297	855	1143	3573
	cc-pV(5+*d*)Z	1028	1095	2300	854	1140	3575
	aug-cc-pV(D+*d*)Z	988	1065	2295	833	1132	3562
	aug-cc-pV(T+*d*)Z	1021	1091	2301	853	1143	3568
	aug-cc-pV(Q+*d*)Z	1025	1093	2302	853	1139	3571
	aug-cc-pV(5+*d*)Z	1028	1095	2302	853	1139	3573
PBE	cc-pVDZ	929	991	2067	784	1084	3368
	cc-pVTZ	963	1025	2091	799	1110	3421
	cc-pVQZ	973	1033	2097	798	1105	3415
	cc-pV5Z	981	1041	2104	800	1099	3413
	cc-pV(D+*d*)Z	949	1004	2059	786	1084	3362
	cc-pV(T+*d*)Z	975	1037	2095	805	1110	3412
	cc-pV(Q+*d*)Z	981	1041	2106	801	1103	3412
	cc-pV(5+*d*)Z	982	1043	2105	800	1099	3412
	aug-cc-pV(D+*d*)Z	950	1015	2116	783	1090	3398
	aug-cc-pV(T+*d*)Z	975	1038	2119	801	1101	3407
	aug-cc-pV(Q+*d*)Z	980	1041	2114	800	1098	3409
	aug-cc-pV(5+*d*)Z	982	1043	2108	800	1098	3411

and Ventura.[29] The tight *d* functions greatly improved the convergence behavior with respect to increasing basis set as shown.

D. Enthalpy of Formation of HSO. For purposes of this study, our interest in examining the enthalpy of formation is in order to assess the potential impact of the tight *d* functions upon calculated enthalpies of formation, rather than provide a recommended route or full discussion of possible means to determine the enthalpy of formation. We have simply selected a series of reactions used (and discussed fully) in previous work, most notably the work by Denis and Ventura using B3LYP and B3PW91 in combination with the cc-pV*x*Z basis sets,[29] as this provides us with a means for comparison for the tight *d*-augmented basis sets.

The seven reactions evaluated include the following:

$$H_2S + SO \rightarrow HSO + HS \quad (1)$$

$$H + SO \rightarrow HSO \quad (2)$$

$$H_2 + 2SO \rightarrow 2HSO \quad (3)$$

$$HS + O \rightarrow HSO \quad (4)$$

$$2HS + O_2 \rightarrow 2HSO \quad (5)$$

$$H + S + O \rightarrow HSO \quad (6)$$

$$H_2 + 2S + O_2 \rightarrow 2HSO \quad (7)$$

In Table 7, the HSO enthalpy of formation determined for each reaction, method, and basis set combination is reported, along with results from previous calculations. For each combination, the enthalpy of formation has been determined by combining enthalpies of reaction with accurately known enthalpies of formation.

Reactions 4−7 are more greatly impacted by the tight *d*-augmented basis sets than reactions 1−3. For example, at the aug-cc-pVDZ level, the tight *d* set results in an overall reduction of the enthalpies of formation of 5 kcal/mol (or greater) as well as a change in sign of the enthalpy (in all cases but reaction 5). In reaction 6 with B3LYP, tight *d* functions result in reduction of the enthalpy of formation by 6.27, 3.86, 2.3, and 0.51 kcal/mol energy at the aug-cc-pVDZ, cc-pVTZ, cc-pVQZ, and cc-pV5Z levels, respectively. Overall, at the quadruple-ζ level, for reactions 4−7, the tight *d* set results in a reduction of ∼2−3 kcal/mol in the enthalpy. This marks a change in the value of cc-pVQZ relative to cc-pV(Q+*d*)Z of 48%, 70%, 36%, and 57% for reactions 4−7, respectively.

Reactions 1−3 are not impacted as significantly by the tight *d* functions. At the B3LYP/aug-cc-pVDZ level, the tight *d* drops the enthalpy of formation determined by reaction 1 by only 0.17 kcal/mol. The changes for reactions 2 and 3 are slightly higher, with differences of 1.37 and 1.33 kcal/mol, respectively. At the quadruple-ζ level, the impact of the tight *d* function is reduced to 0.06, 0.58, and 0.54 kcal/mol for reactions 1−3. As compared with the cc-pV(Q+*d*)Z enthalpy of formation, this marks percentage differences of 1%, 13%, and 13% for the three reactions, indicating the smaller impact of the tight *d* functions.

Though the tight *d* functions do have an impact upon the overall convergence rate of the enthalpy of formation and also can have a dramatic impact upon the value of the enthalpy when lower level basis sets (through quadruple-ζ for reactions 4−7)

TABLE 5: Energy Differences (with Respect to HSO) of HSO and HOS[e]

method	basis set	ΔE_e (HOS−HSO) kcal/mol	ΔE_o (HOS−HSO) kcal/mol
B3LYP	cc-pVDZ	−4.25	−2.41
	cc-pVTZ[a]	−0.26	1.55
	cc-pVQZ[a]	1.41	3.20
	cc-pV5Z[a]	2.87	4.64
	cc-pV(D+*d*)Z	−0.42	1.36
	cc-pV(T+*d*)Z	2.21	3.99
	cc-pV(Q+*d*)Z	2.85	4.61
	cc-pV(5+*d*)Z	3.17	4.92
	aug-cc-pV(D+*d*)Z	0.86	2.65
	aug-cc-pV(T+*d*)Z	2.92	4.66
	aug-cc-pV(Q+*d*)Z	3.09	4.84
	aug-cc-pV(5+*d*)Z	3.23	4.98
B3PW91	cc-pVDZ	−3.65	−1.82
	cc-pVTZ[a]	−0.41	2.34
	cc-pVQZ[a]	2.01	3.82
	cc-pV5Z[a]	3.47	5.23
	cc-pV(D+*d*)Z	0.24	2.01
	cc-pV(T+*d*)Z	2.90	4.68
	cc-pV(Q+*d*)Z	3.48	5.24
	cc-pV(5+*d*)Z	3.78	5.54
	aug-cc-pV(D+*d*)Z	1.66	3.44
	aug-cc-pV(T+*d*)Z	3.52	5.27
	aug-cc-pV(Q+*d*)Z	3.67	5.43
	aug-cc-pV(5+*d*)Z	3.83	5.59
PBE	cc-pVDZ	−1.94	−0.15
	cc-pVTZ	1.77	3.56
	cc-pVQZ	3.38	5.14
	cc-pV5Z	4.90	6.62
	cc-pV(D+*d*)Z	1.88	3.59
	cc-pV(T+*d*)Z	4.20	5.95
	cc-pV(Q+*d*)Z	4.83	6.55
	cc-pV(5+*d*)Z	5.21	6.92
	aug-cc-pV(D+*d*)Z	3.39	5.11
	aug-cc-pV(T+*d*)Z	4.98	6.68
	aug-cc-pV(Q+*d*)Z	5.13	6.83
	aug-cc-pV(5+*d*)Z	5.28	6.99
CASSCF[b]	aug-cc-pVDZ	−3.3	−1.9
	cc-pVTZ	0.4	1.9
	cc-pVQZ	2.2	3.7
	cc-pV5Z	3.1	4.6
	CBS limit[c]		5.41
CASSCF+1+2[b]	aug-cc-pVDZ	−4.4	−3.0
	cc-pVTZ	−0.8	1.0
	cc-pVQZ	1.5	3.1
	cc-pV5Z	2.6	4.2
	CBS limit[c]		5.42
CCSD(T)[d]	cc-pVDZ	−6.37	−4.49
	cc-pVTZ	−2.26	−0.41
	cc-pVQZ	−0.15	1.70
	cc-pV5Z	1.49	3.34
	cc-pV(D+*d*)Z	−2.76	−0.95
	cc-pV(T+*d*)Z	0.01	1.82
	cc-pV(Q+*d*)Z	1.16	2.97
	cc-pV(5+*d*)Z	1.76	3.57
	CBS limit	2.4	4.2

[a] Reference 29. [b] Reference 20. [c] A cc-pVQZ geometry was used. [d] Reference 1. [e] ΔE_e represents the energy difference without including the zero point correction while ΔE_o represents the energy difference including the zero point correction. A positive value indicates that the HSO isomer is more stable than HOS.

are used, at the quintuple-ζ level, the conclusions reached in the earlier study by Denis and Ventura regarding the magnitude of enthalpies of formation calculated via reactions 1−7 remain the same. The calculated enthalpies of formation overall result in two different ranges of values. From reactions 1, 4, and 6, B3LYP/aug-cc-pV(5+*d*)Z values of −6.29, −6.36, and −7.06 kcal/mol emerge, while for reactions 2, 3, 5, and 7, values of −4.83, −4.42, −4.49, and −4.73 kcal/mol result. For B3PW91,

TABLE 6: Kohn−Sham Limits of the Energy Differences (with Respect to HSO) of HSO and HOS[a]

		ΔE_o(HOS−HSO) kcal/mol		
method	extrapolation	cc-pVxZ	cc-pV(*x*+*d*)Z	aug-cc-pV(*x*+*d*)Z
B3LYP	KS_{DTQ5}	5.81	4.95	4.94
	KS_{DTQ}	4.38	4.80	4.86
	KS_{DT}	3.22	5.70	6.15
	KS_{TQ}	4.40	5.06	4.97
	KS_{Q5}	6.15	5.25	5.13
B3PW91	KS_{DTQ5}	6.04	5.55	5.54
	KS_{DTQ}	4.64	5.39	5.45
	KS_{DT}	4.09	6.49	6.75
	KS_{TQ}	4.90	5.65	5.55
	KS_{Q5}	6.71	5.85	5.76
PBE	KS_{DTQ5}	7.97	6.97	6.94
	KS_{DTQ}	6.31	6.75	6.85
	KS_{DT}	5.12	7.76	8.20
	KS_{TQ}	4.55	6.99	6.94
	KS_{Q5}	6.49	7.31	7.16

[a] ΔE_o represents the energy difference including zero point correction. A positive value indicates that the HSO isomer is more stable than HOS.

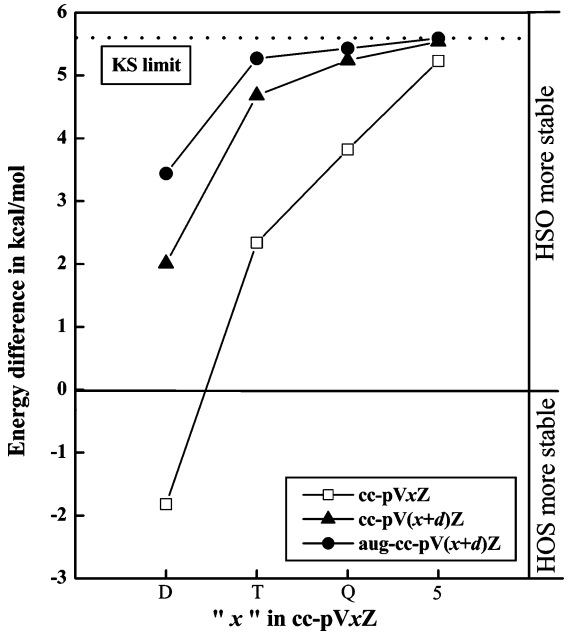

Figure 1. Relative energies of the HSO and HOS isomers obtained from B3PW91 calculations with the cc-pV(*x*+d)Z and aug-cc-pV(*x*+d)Z basis sets. cc-pV*x*Z results from Denis and Ventura[29] (represented by the □ − though the cc-pVDZ result is from the present study) have been included for comparison.

all predicted enthalpies of formation fall in three ranges, ∼ −4 kcal/mol for reactions 2 and 5, ∼ −6 kcal/mol for reactions 1, 3, and 7, and ∼ −7 kcal/mol for reactions 4 and 6. Interestingly, the enthalpies of formation determined using PBE differ substantially, based upon the reaction used in the determination. A very large enthalpy of formation (∼ −20 kcal/mol) is obtained based upon reactions 4 and 6, while reactions 1 and 2 result in similar enthalpies as those determined by B3PW91. These values are not surprising, as PBE has been shown to perform poorly in predicting thermochemical data, including enthalpies of formation, for a large range of molecular systems.[53,54] Xantheas and Dunning suggest a value of −4.2 kcal/mol based upon their CASSCF results which were obtained using the standard correlation consistent basis sets.[19] Esseffar also suggests a value of −4.2 kcal/mol, using QCISD(T).[31] Recently, Denis determined a value of −5.2 kcal/mol using CCSD(T) with the aug-cc-pV(*x*+*d*)Z basis sets.[55] All above theoretical results are larger

TABLE 7: Estimated Enthalpies of Formation for HSO in kcal/mol

method/ basis set	reaction 1 $H_2S + SO \rightarrow$ HSO + HS	reaction 2 $H + SO \rightarrow$ HSO	reaction 3 $H_2 + 2SO \rightarrow$ 2HSO	reaction 4 $HS + O \rightarrow$ HSO	reaction 5 $2HS + O_2 \rightarrow$ 2HSO	reaction 6 $H + S + O \rightarrow$ HSO	reaction 7 $H_2 + 2S + O_2 \rightarrow$ 2HSO
B3LYP/							
aug-cc-pVDZ[a]	−6.05	−2.39	−3.59	5.33	6.48	6.00	5.98
cc-pVTZ[a]	−5.43	−3.04	−2.70	−0.41	1.31	−1.00	1.05
cc-pVQZ[a]	−5.98	−3.97	−3.59	−3.06	−1.17	−4.13	−1.74
cc-pV5Z[a]	−6.38	−4.61	−4.23	−5.02	−3.23	−6.38	−4.21
cc-pV(D+*d*)Z	−4.50	−1.71	−2.75	3.48	5.14	4.64	5.31
cc-pV(T+*d*)Z	−5.62	−3.99	−3.63	−4.49	−2.76	−4.86	−2.72
cc-pV(Q+*d*)Z	−6.04	−4.55	−4.13	−5.84	−3.95	−6.43	−4.08
cc-pV(5+*d*)Z	−6.23	−4.75	−4.34	−6.26	−4.47	−6.89	−4.64
aug-cc-pV(D+*d*)Z	−6.22	−3.76	−4.92	−0.64	0.51	−0.27	−0.22
aug-cc-pV(T+*d*)Z	−6.25	−4.67	−4.36	−5.35	−3.92	−6.00	−4.21
aug-cc-pV(Q+*d*)Z	−6.27	−4.78	−4.39	−6.12	−4.27	−6.84	−4.56
aug-cc-pV(5+*d*)Z	−6.29	−4.83	−4.42	−6.36	−4.49	−7.06	−4.73
B3PW91/							
aug-cc-pVDZ[a]	−5.81		−4.54	4.25	6.02		4.90
cc-pVTZ[a]	−5.26		−3.92	−1.53	0.81		−0.24
cc-pVQZ[a]	−5.76		−4.68	−4.13	−1.58		−2.99
cc-pV5Z[a]	−6.12		−5.28	−6.09	−3.61		−5.31
cc-pV(D+*d*)Z	−4.41	−1.70	−3.88	2.80	4.63	4.47	4.10
cc-pV(T+*d*)Z	−5.46	−3.71	−4.82	−5.66	−3.31	−5.34	−4.10
cc-pV(Q+*d*)Z	−5.84	−4.16	−5.22	−6.95	−4.39	−6.79	−5.30
cc-pV(5+*d*)Z	−5.99	−4.33	−5.40	−7.36	−4.87	−7.24	−5.82
aug-cc-pV(D+*d*)Z	−6.01	−3.58	−5.88	−1.84	−0.08	−0.85	−1.39
aug-cc-pV(T+*d*)Z	−5.98	−4.26	−5.41	−6.52	−4.37	−6.37	−5.38
aug-cc-pV(Q+*d*)Z	−6.01	−4.34	−5.42	−7.19	−4.66	−7.08	−5.64
aug-cc-pV(5+*d*)Z	−6.04	−4.40	−5.46	−7.44	−4.88	−7.36	−5.88
PBE/							
cc-pVDZ	−2.39	0.56	−2.91	−6.54	5.75	−4.74	4.08
cc-pVTZ	−3.81	−2.12	−4.44	−15.33	−3.30	−15.11	−5.40
cc-pVQZ	−4.46	−3.02	−5.35	−17.75	−5.70	−17.90	−8.18
cc-pV5Z	−4.93	−3.72	−6.07	−19.58	−7.72	−19.99	−10.50
cc-pV(D+*d*)Z	−3.03	−1.00	−4.46	−11.33	0.96	−10.47	−1.65
cc-pV(T+*d*)Z	−4.31	−3.12	−5.44	−18.47	−6.44	−18.79	−9.08
cc-pV(Q+*d*)Z	−4.77	−3.62	−5.95	−19.66	−7.61	−20.12	−10.40
cc-pV(5+*d*)Z	−4.98	−3.83	−6.18	−19.96	−8.10	−20.45	−10.95
aug-cc-pV(D+*d*)Z	−4.85	−3.05	−6.73	−15.15	−3.80	−14.88	−7.21
aug-cc-pV(T+*d*)Z	−4.96	−3.77	−6.19	−19.14	−7.61	−19.61	−10.52
aug-cc-pV(Q+*d*)Z	−5.01	−3.86	−6.23	−19.83	−7.93	−20.34	−10.82
aug-cc-pV(5+*d*)Z	−5.05	−3.92	−6.28	−20.04	−8.12	−20.57	−11.03
QCISD(T)/6-311++G(5d2f,2p)[b]	−4.71	−4.71		−4.40		−4.30	
CASSCF+1+2/cc-pV5Z[c]		−4.11					
CASSCF+1+2/CBS limit[c]		−4.21					
CI/CBS limit[c]		−5.40					
G2[b]	−5.40	−5.62		−3.11		−3.01	
G2*[b]	−5.62	−5.90		−2.51		−2.41	
G2**[d]	−5.40	−5.90		−5.90		−4.57	
experimental	$\Delta H_{f,o}^{o}$						
exp[e]	14.9						
exp [f]	−3.0						
exp[g]	−1.4 ± 2.0						
exp[h]	−1.6 ± 0.7						
exp[i]	< −3.7						

[a] Reference 29. [b] Reference 31. [c] Reference 20. [d] Reference 32. [e] Reference 52. [f] Reference 17. [g] Reference 58. [h] Reference 59. [i] Reference 56.

than a recently experimental enthalpy of formation (−3.0 kcal/mol) by Balucani.[56]

E. Reaction Barrier to HSO → HOS. In a previous study, CASSCF+1+2 was used in combination with cc-pVTZ and cc-pVQZ to determine the reaction barrier for the HSO/HOS isomerization.[19] A substantial barrier was observed, which helps to explain why only HSO has been observed experimentally. In this study, DFT was used with the standard and tight *d*-augmented correlation consistent basis sets in order to assess the usefulness and impact of DFT and tight *d* functions in determining the barrier to isomerization, which is reported in Table 8. Additionally, the structure and harmonic frequencies for the transition state are shown in Table 8 and are compared with previous CASSCF+1+2 calculations.

The tight *d*-augmented functions have an expected effect upon the barrier to isomerization—convergence in the barrier occurs more quickly than for the standard basis sets. For all three functionals, the barrier has nearly reached convergence at the quadruple-ζ level when the tight *d*-augmented sets are used, whereas this does not occur until the quintuple-ζ level for the standard basis sets. The bond S−O and H−S bond distances determined for the transition state are slightly longer than those shown by CASSCF+1+2/cc-pVQZ. The bond angle is ∼1−2° larger using DFT.

IV. Conclusions

The use of the cc-pV(*x*+*d*)Z and aug-cc-pV(*x*+*d*)Z basis sets in combination with B3LYP, B3PW91, and PBE for sulfur

TABLE 8: Structure of the Transition State and the Barrier for the HSO → HOS Isomerization with Respect to HSO

method	basis set	R (S−O) Å	R (H−S) Å	Φ (H−S−O) deg	ΔE kcal/mol
B3LYP	cc-pVDZ	1.703	1.435	51.03	40.77
	cc-pVTZ	1.665	1.435	50.99	45.59
	cc-pVQZ	1.657	1.437	50.89	46.93
	cc-pV5Z	1.650	1.438	50.84	48.00
	cc-pV(D+*d*)Z	1.684	1.432	51.04	43.83
	cc-pV(T+*d*)Z	1.655	1.434	50.96	47.52
	cc-pV(Q+*d*)Z	1.651	1.436	50.88	48.02
	cc-pV(5+*d*)Z	1.649	1.438	50.83	48.22
	aug-cc-pV(D+*d*)Z	1.678	1.447	50.59	45.06
	aug-cc-pV(T+*d*)Z	1.653	1.439	50.78	47.71
	aug-cc-pV(Q+*d*)Z	1.650	1.438	50.81	48.05
	aug-cc-pV(5+*d*)Z	1.649	1.438	50.81	48.22
B3PW91	cc-pVDZ	1.689	1.429	51.40	40.46
	cc-pVTZ	1.653	1.429	51.32	45.00
	cc-pVQZ	1.645	1.431	51.22	46.23
	cc-pV5Z	1.639	1.431	51.16	47.26
	cc-pV(D+*d*)Z	1.672	1.426	51.41	43.52
	cc-pV(T+*d*)Z	1.643	1.428	51.28	46.90
	cc-pV(Q+*d*)Z	1.639	1.430	51.19	47.31
	cc-pV(5+*d*)Z	1.638	1.431	51.15	47.49
	aug-cc-pV(D+*d*)Z	1.666	1.440	50.89	44.58
	aug-cc-pV(T+*d*)Z	1.641	1.432	51.11	46.99
	aug-cc-pV(Q+*d*)Z	1.639	1.432	51.13	47.31
	aug-cc-pV(5+*d*)Z	1.638	1.432	51.13	47.49
PBE	cc-pVDZ	1.716	1.436	52.11	35.26
	cc-pVTZ	1.681	1.440	51.51	39.78
	cc-pVQZ	1.674	1.442	51.31	41.04
	cc-pV5Z	1.669	1.443	51.15	42.12
	cc-pV(D+*d*)Z	1.700	1.434	51.96	38.20
	cc-pV(T+*d*)Z	1.672	1.439	51.42	41.64
	cc-pV(Q+*d*)Z	1.668	1.441	51.24	42.12
	cc-pV(5+*d*)Z	1.667	1.443	51.13	42.34
	aug-cc-pV(D+*d*)Z	1.694	1.452	50.94	39.61
	aug-cc-pV(T+*d*)Z	1.670	1.444	51.07	41.90
	aug-cc-pV(Q+*d*)Z	1.668	1.444	51.09	42.20
	aug-cc-pV(5+*d*)Z	1.667	1.444	51.09	42.37
CASSCF+1+2[a]	cc-pVTZ	1.677	1.355	54.92	44.5
	cc-pVQZ	1.630	1.426	49.88	46.3

[a] Reference 20.

species such as HSO and HOS can be important, particularly for the lower level basis sets. For structures, the impact upon the bond lengths and angles of these structures is slight. However, the sets do enable a converged geometry to be ascertained using a lower level basis set. In terms of a description of the relative energies of the isomers, the tight *d* functions enable the correct prediction that HSO is more stable than HOS to occur with simply a double-ζ level basis set and yield a relative energy of HSO and HOS that is in good agreement with previous MRCI calculations by Xantheas and Dunning. For the enthalpy of formation, the tight *d*-augmented basis sets can have a significant impact upon the enthalpies, even for a quadruple-ζ level basis set. The level of impact seems to be heavily based upon reaction used to determine the enthalpy. Overall, the use of the cc-pV(*x*+*d*)Z and aug-cc-pV(*x*+*d*)Z basis sets is important in the determination of energetics, including thermochemical properties such as enthalpies, and is recommended, particularly when lower level basis sets will be employed.

Acknowledgment. This work was performed at the University of North Texas. The authors gratefully acknowledge support from a National Science Foundation CAREER Award (CHE-0239555) and the University of North Texas Faculty Research Grant Program. Computer resources were provided via support from the National Science Foundation (CHE-0342824) and from the National Computational Science Alliance (#CHE010021). Additional computational support was provided by Academic Computing Services at the University of North Texas on the UNT Research Cluster.

References and Notes

(1) Wilson, A. K.; Dunning, T. H., Jr. *J. Phys. Chem. A* **2004**, *108*, 3129.
(2) Dunning, T. H., Jr. *J. Chem. Phys.* **1989**, *90*, 1007.
(3) Woon, D. E.; Dunning, T. H., Jr. *J. Chem. Phys.* **1993**, *98*, 1358.
(4) Woon, D. E.; Dunning, T. H., Jr. *J. Chem. Phys.* **1995,** *103*, 4572.
(5) Wilson, A. K.; van Mourik, T.; Dunning, T. H., Jr. *J. Mol. Struct. (THEOCHEM)* **1996**, *388*, 339.
(6) Wilson, A. K.; Woon, D. E.; Peterson, K. A.; Dunning, T. H., Jr. *J. Chem. Phys.* **1999**, *110*, 7667.
(7) van Mourik, T.; Dunning, T. H., Jr. *Int. J. Quantum Chem.* **2000**, *76*, 205.
(8) Peterson, K. A.; Dunning, T. H., Jr. *J. Chem. Phys.* **2002**, *117*, 10548.
(9) Kendall, R. A.; Dunning, T. H., Jr.; Harrison, R. J. *J. Chem. Phys.* **1992**, *96*, 6796.
(10) Peterson, K. A. *J. Chem. Phys.* **2003**, *119*, 11099.
(11) Peterson, K. A.; Figgen, D.; Goll, E.; Stoll, H.; Dolg, M. *J. Chem. Phys.* **2003**, *119*, 11113.
(12) Dunning, T. H., Jr.; Peterson, K. A.; Wilson, A. K. *J. Chem. Phys.* **2001**, *114*, 9244.
(13) Luke, B. T.; McLean, A. D. *J. Phys. Chem.* **1985**, *89*, 4592.
(14) Moore Plummer, P. L. *J. Chem. Phys.* **1990**, *92*, 6627.
(15) Sannigrahi, A. B.; Thunemann, K. H.; Peyerimhoff, S. D.; Buenker, R. J. *J. Chem. Phys.* **1977**, *20*, 55.
(16) Sannigrahi, A. B.; Peyerimhoff, S. D.; Buenker, R. J. *J. Chem. Phys.* **1977**, *20*, 381.
(17) Slagle, I. R.; Graham, R. G.; Gutman, D. *Int. J. Chem. Kinet.* **1976**, *8*, 451.
(18) Kawasaki, M.; Kasatani, K.; Tanahashi, S.; Sato, H.; Fujimura, Y. *J. Chem. Phys.* **1983**, *78*, 7146.

(19) Xantheas, S. S.; Dunning, T. H., Jr. *J. Phys. Chem.* **1993**, *97*, 18.
(20) Xantheas, S. S.; Dunning, T. H., Jr. *J. Phys. Chem.* **1993**, *97*, 6616.
(21) Bauschlicher, C. W.; Partridge, H. *Chem. Phys. Lett.* **1995**, *240*, 533.
(22) Purvis, G. D.; Bartlett, R. J. *J. Chem. Phys.* **1982**, *76*, 1910.
(23) Raghavachari, K.; Trucks, G. W.; Pople, J. A.; Head-Gordon, M. *Chem. Phys. Lett.* **1989**, *157*, 479.
(24) Martin, J. M. L. *J. Chem. Phys.* **1998**, *108*, 2791.
(25) Martin, J. M. L.; Uzan, O. *Chem. Phys. Lett.* **1998**, *282*, 16.
(26) Wang, N. X.; Wilson, A. K. *J. Phys. Chem. A* **2003**, *107*, 6720.
(27) Wilson, A. K.; Dunning, T. H., Jr. *J. Chem. Phys.* **2003**, *119*, 11712.
(28) Bell, R. D.; Wilson, A. K. *Chem. Phys. Lett.* **2004**, *394*, 105.
(29) Denis, P. A.; Ventura, O. N. *Int. J. Quantum Chem.* **2000**, *80*, 439.
(30) Espinosa-Garcia, J.; Corchado, J. C. *Chem. Phys. Lett.* **1994**, *218*, 128.
(31) Esseffar, M.; Mo, O.; Yanez, M. *J. Chem. Phys.* **1994**, *101*, 2175.
(32) Wilson, C.; Hirst, D. M. *J. Chem. Soc., Faraday Trans.* **1994**, *90*, 3051.
(33) Goumri, A.; Laakso, D.; Rocha, J. R.; Smith, C. E.; Marshall, P. *J. Chem. Phys.* **1995**, *102*, 161.
(34) Decker, B. K.; Adams, N. G.; Babcock, L. M.; Crawford, T. D.; Schaefer, H. F., III *J. Phys. Chem. A* **2000**, *104*, 4636.
(35) Becke, A. D. *J. Chem. Phys.* **1993**, *98*, 5648.
(36) Lee, C.; Yang, W.; Parr, R. G. *Phys. Rev. B* **1988**, *37*, 785.
(37) Perdew, J. P.; Chevary, J. A.; Vosko, S. H.; Jackson, K. A.; Pederson, M. R.; Singh, D. J.; Fiolhas, C. *Phys. Rev. B* **1992**, *46*, 6671.
(38) Perdew, J. P.; Burke, K.; Ernzerhof, M. *Phys. Rev. Lett.* **1996**, *77*, 3865.
(39) Perdew, J. P.; Burke, K.; Ernzerhof, M. *Phys. Rev. Lett.* **1997**, *78*, 1396.
(40) Frisch, M. J.; Trucks, G. W.; Schlegel, H. B.; Scuseria, G. E.; Robb, M. A.; Cheeseman, J. R.; Zakrzewski, V. G.; Montgomery, J. A., Jr.; Stratmann, R. E.; Burant, J. C.; Dapprich, S.; Millam, J. M.; Daniels, A. D.; Kudin, K. N.; Strain, M. C.; Farkas, O.; Tomasi, J.; Barone, V.; Cossi, M.; Cammi, R.; Mennucci, B.; Pomelli, C.; Adamo, C.; Clifford, S.; Ochterski, J.; Petersson, G. A.; Ayala, P. Y.; Cui, Q.; Morokuma, K.; Salvador, P.; Dannenberg, J. J.; Malick, D. K.; Rabuck, A. D.; Raghavachari, K.; Foresman, J. B.; Cioslowski, J.; Ortiz, J. V.; Baboul, A. G.; Stefanov, B. B.; Liu, G.; Liashenko, A.; Piskorz, P.; Komaromi, I.; Gomperts, R.; Martin, R. L.; Fox, D. J.; Keith, T.; Al-Laham, M. A.; Peng, C. Y.; Nanayakkara, A.; Challacombe, M.; Gill, P. M. W.; Johnson, B.; Chen, M.; Wong, M. W.; Andres, J. L.; Gonzalez, C.; Head-Gordon, M.; Replogle, E. S.; Pople, J. A. Gaussian 98, Revision A, 11th ed.; Gaussian, Inc.: Pittsburgh, PA, 2001.
(41) Frisch, M. J.; Trucks, G. W.; Schlegel, H. B.; Scuseria, G. E.; Robb, M. A.; Cheeseman, J. R.; Montgomery, J. A., Jr.; Vreven, T.; Kudin, K. N.; Burant, J. C.; Millam, J. M.; Iyengar, S. S.; Tomasi, J.; Barone, V.; Mennucci, B.; Cossi, M.; Scalmani, G.; Rega, N.; Petersson, G. A.; Nakatsuji, H.; Hada, M.; Ehara, M.; Toyota, K.; Fukuda, R.; Hasegawa, J.; Ishida, M.; Nakajima, T.; Honda, Y.; Kitao, O.; Nakai, H.; Klene, M.; Li, X.; Knox, J. E.; Hratchian, H. P.; Cross, J. B.; Bakken, V.; Adamo, C.; Jaramillo, J.; Gomperts, R.; Stratmann, R. E.; Yazyev, O.; Austin, A. J.; Cammi, R.; Pomelli, C.; Ochterski, J. W.; Ayala, P. Y.; Morokuma, K.; Voth, G. A.; Salvador, P.; Dannenberg, J. J.; Zakrzewski, V. G.; Dapprich, S.; Daniels, A. D.; Strain, M. C.; Farkas, O.; Malick, D. K.; Rabuck, A. D.; Raghavachari, K.; Foresman, J. B.; Ortiz, J. V.; Cui, Q.; Baboul, A. G.; Clifford, S.; Cioslowski, J.; Stefanov, B. B.; Liu, G.; Liashenko, A.; Piskorz, P.; Komaromi, I.; Martin, R. L.; Fox, D. J.; Keith, T.; Al-Laham, M. A.; Peng, C. Y.; Nanayakkara, A.; Challacombe, M.; Gill, P. M. W.; Johnson, B.; Chen, W.; Wong, M. W.; Gonzalez, C.; Pople, J. A. Gaussian 03, Revison C.02 ed.; Gaussian, Inc.: Wallingford CT, 2004.
(42) Clabo, D. A.; Allen, W. D.; Remington, R. B.; Yamaguchi, Y.; Schaefer, H. F., III *Chem. Phys.* **1988**, *123*, 187.
(43) Miller, W. H.; Handy, N. C.; Adams, J. E. *J. Chem. Phys.* **1980**, *72*, 99.
(44) Page, M.; McIver, J. W., Jr. *J. Chem. Phys.* **1988**, *88*, 922.
(45) Page, M.; Doubleday: C.; McIver, J. W., Jr. *J. Chem. Phys.* **1990**, *93*, 5634.
(46) Senekowitsch, J. Ph.D. Thesis, Universität Frankfurt, Germany, 1988.
(47) Feller, D. *J. Chem. Phys.* **1992**, *96*, 6104.
(48) Kupka, T.; Ruscic, B.; Botto, R. E. *J. Phys. Chem. A* **2002**, *106*, 10396.
(49) Kupka, T.; Ruscic, B.; Botto, R. *Solid State Nucl. Magn. Reson.* **2003**, *23*, 145.
(50) Raymond, K. S.; Wheeler, R. A. *J. Comput. Chem.* **1999**, *20*, 207.
(51) Halkier, A.; Helgaker, T.; Jogensen, P.; Klopper, W.; Koch, H.; Olsen, J.; Wilson, A. K. *Chem. Phys. Lett.* **1998**, *286*, 243.
(52) Ohashi, N.; Kakimoto, M.; Saito, S.; Hirota, E. *J. Mol. Spectrosc.* **1980**, *84*, 204.
(53) Xu, X.; Goddard, W. A. *J. Chem. Phys.* **2004**, *121*, 4068.
(54) Rabuck, A. D.; Scuseria, G. E. *Chem. Phys. Lett.* **1999**, *309*, 450.
(55) Denis, P. A. *Chem. Phys. Lett.* **2005**, *402*, 289.
(56) Balucani, N.; Stranges, D.; Casavecchia, P.; Volpi, G. G. *J. Chem. Phys.* **2004**, *120*, 9571.
(57) Schurath, U.; Weber, M.; Becker, K. H. *J. Chem. Phys.* **1977**, *67*, 110.
(58) Davidson, F. E.; Clemo, A. R.; Duncan, D. L.; Browet, R. J.; Hobson, J. H.; Grice, R. *Mol. Phys.* **1985**, *46*, 33.
(59) Balucani, N.; Casavecchia, P.; Stranges, D.; Volpi, G. G. *Chem. Phys. Lett.* **1993**, *211*, 469.